INTERNATIONAL JOURNAL OF INTEGRATED ENGINEERING
ISSN: 2229-838X e-ISSN: 2600-7916

IJIE

Vol. 17 No. 8 (2025) 65-77
https://publisher.uthm.edu.my/ojs/index.php/ijie

The Influence of Carbon Powder on the Physical, Mechanical and Absorption Properties of Carbon Foam from Natural Precursor Starch

Mohamed Nasrul Mohamed Hatta[1]*, Muhammad Shamim Amir Mohd Nasir[1,2], Kamarul Azhar Kamarudin[3]

[1] *Nano Structure and Surface Modification Research Group, Faculty of Mechanical and Manufacturing Engineering, Universiti Tun Hussein Onn Malaysia, 86400 Parit Raja, Batu Pahat, Johor, MALAYSIA*

[2] *Favelle Favco Cranes (M) Sdn Bhd, 42 Persiaran Bunga Tanjung, Senawang Industrial Park, 70400 Seremban, Negeri Sembilan, MALAYSIA*

[3] *Crashworthiness and Collision Research Group (COLORED), Faculty of Mechanical and Manufacturing Engineering, Universiti Tun Hussein Onn Malaysia, 86400 Parit Raja, Batu Pahat, Johor, MALAYSIA*

*Corresponding Author: mnasrul@uthm.edu.my
DOI: https://doi.org/10.30880/ijie.2025.17.08.007

Article Info

Received: 1 July 2025
Accepted: 18 November 2025
Available online: 31 December 2025

Keywords

Carbon foam, natural carbon precursor, blowing method, mechanical properties, absorption properties

Abstract

This study was fabricated the starch-based carbon foam with sodium borate as the blowing agent and reinforced with carbon powder. The effect of carbon powder on the physical, mechanical and adsorption properties was investigated. The temperature of foaming and carbonization was fixed but the carbon powder percentage was varied in the range between 2wt% to 8wt%. The physical properties of the carbon foam analysed by the density and porosity, pore morphology was analysed by using Scanning Electron Microscopy (SEM) and carbon bonding was observed through Fourier-infrared Spectroscopy (FTIR). The percentage of the carbon powder inside the carbon foam influence the properties of the carbon foam. The higher the content of the carbon powder, the higher the bulk density but low porosity. The results of the pore morphology using the SEM proved the size of the pore decreases as the carbon powder percentage increase inside the carbon foam. The FTIR analysis shows the carbon bonding. Furthermore, the maximum stress and maximum force applied also rises as the carbon powder increases. The highest value of maximum stress was achieved by carbon foam with 8wt% of carbon powder which is 1.71345 N/mm^2 respectively. Since the bulk density is higher, the oil adsorption lower due to small porosity of the carbon foam. The characteristic remains for all parameters when the reusability test implemented by burning the carbon foam. The objectives of the study achieved and the effect of carbon powder to carbon foam proven.

1. Introduction

Carbon foam is a highly porous carbonaceous structural material with an exceptional of material properties with less density but high in mechanical properties [1]. Carbon foams are high-quality carbon products employed for thermal management due to their customizable thermal conductivity, which can range from insulation to heat transfer. This versatility arises from their three-dimensional networks, shapes, sizes, cell parameters, and carbon

structures [2]. It's applications in various fields, including aerospace, energy storage, thermal management, and environmental remediation [3,4]. Besides that, carbon foam has capability to be used as absorbent material [5]. Due to the large amount of oily wastewater generated by global industrial manufacturing and daily living, the separation of oily wastewater is an important matter. The carbon foams with large pores, a thin structure, and a low density can have a significant capacity for emulsifying oil adsorption and have enough storage space for this process [6].

Carbon powder that acts as the reinforcement agent can be defined as the elemental carbon that is produced by the combustion or thermal decomposition of gas or liquid hydrocarbons. The specific surface area of carbon powder is very high, providing it with excellent adsorption capabilities [7]. With the mixture of the starch, it is a good combination to form carbon foam and adsorption abilities. The current trend in this industry, the carbon foam was produced from hydrocarbon material such as coal and tar [8]. This material was related to environmental issues. Therefore, natural precursors are attracted to be explored as substitution material for future sustainable industry. Starch is one of the materials with high value of glucose units which are good agents for fabricating carbon foam. Starch is widely regarded as a green, cost-effective, and renewable natural polymer that serves as a relatively natural precursor for producing high yield porous carbon materials with fewer impurities [9].

For this study, carbon foam was fabricated from natural precursor starch. The carbon powder was added as reinforcement at different composition in the structure. The objectives of this study are to produce carbon foams reinforced with carbon powder. The influence of carbon powder on the physical and mechanical properties was investigated including the capability of the carbon foam to be used as absorbent material.

2. Materials Preparation

2.1 Fabrication of Carbon Foam

The fabrication process of carbon foam started with the mixing process of the materials for each parameter. The materials prepared are starch, carbon powder, distilled water and sodium borate. The percentage of the materials was divided into four which are 74% for starch, 24.5% of distilled water, 1.5% of blowing agent, sodium borate. The carbon powder percentages were 0%, 2%, 4%, 6% and 8%. The percentage of starch was decreased as the percentage of the carbon powder added to specific parameter. The mixture then poured into the cube shaped aluminum mold with 2cm x 2cm x 2cm sized. The samples were undergoing a foaming process for 6 hours at 200°C temperature. The mixture must be remixed if the samples were fractured and cracked. Next process was carbonization process for 80 minutes at 1000°C under argon atmosphere. These samples were named as Table 1.

Table 1 *The name of samples according to composition of carbon powder*

Name of Sample	Composition of Carbon (wt%)
CFA	0
CFB	2
CFC	4
CFD	6
CFE	8

2.2 Density and Porosity

The value density and porosity of the carbon foam must be analysed to define the interrelation between physical and mechanical properties. The difference of the density and porosity might be caused by the carbon powder that were added to each sample in different amount. The parameter of temperature of the making process might not affected the density and porosity because the temperature value was fixed to the best temperature. The density and pore volume of the carbon foam will be determined by Archimedes Principle. The test of the carbon foam will be run by using the laboratory balance. Once the weight of the samples is obtained, the percentage of density and the porosity will be calculated to achieve the full analysis. The Equation (1) and Equation (2) below are used to calculate the percentage of density and porosity [10].

$$Bulk\ Density, B = \frac{D}{W - S} \quad (1)$$

Int. Journal of Integrated Engineering Vol. 17 No. 8 (2025) p. 65-77

$$Porosity\ (\%) = \left(\frac{W - D}{W - S}\right) \times 100 \quad (2)$$

B = Bulk Density (kgm^{-3})
D = Dry weight of sample (kg)
W = Wet weight of sample (kg)
S = Submerged weight of sample (kg)

2.3 Pore Morphology and Elemental Analysis

Pore morphology was observed to analyze the characterization of the carbon foam by using Scanning Electron Microscope (SEM). The characterization of the carbon foam consists of microstructure morphology and chemical composition. SEM was used to capture and generate images of the grain structure of the carbon foam in deeper scale. It is also used to identify with a closer look and visualize the element and other features of the carbon foam such as shape, distribution and the size of pores. The voltage used for this testing is 10kV. The magnifications observed were 35x, 100x, 300x, 500x and 1000x. The size of the sample in the diameter of 1cm with flat surface on top. The mode of the scanning was secondary electron with elemental scanning. No coating was applied to the sample since the carbon is conductor. Elemental analysis was implemented by Energy Dispersive X-Ray (EDX). It was used to obtain the element composition inside the carbon foam by scanning the area at pore wall. The EDX scanned the composition by using 500x magnification of SEM. The results obtained in the percentage of the element composition and the graph shows the peak percentages.

2.4 Carbon Bonding Analysis

In this test, the microstructure and chemical characterization of the carbon foam was observed by using the Fourier-infrared Spectroscopy (FTIR). FTIR can identify and observe the chemical characterization based on their infrared adsorption or transmission spectra. It also can observe organic, polymeric, and inorganic materials. The chemical characterization might change due to the different amounts of carbon powder added. Any changing in the material's composition or the presence of contaminants is clearly detected by a change in the characteristic pattern of absorption bands. The result of this test was achieved with the graphical result that was analysed by the FTIR machine.

2.5 Compression Test

The compression test is a crucial test to determine the carbon foam's behavior when pressure or load impact on the carbon foam. The was done by using Universal Testing Equipment (UTM). The compression test used the standard of ASTM D695 [11]. The force was applied on two opposites side of the carbon foam cube shaped with size of 1.5cm x 1.5cm x 1.5cm. The carbon foams were compressed until they reached failure. The compressive strength of the carbon foams was determined by the stress vs strain graph.

2.5 Oil Absorption

The oil adsorption of carbon foam was evaluated by the percentage changes of mass of carbon foam. Weigh the sample of carbon foam to get the initial weight before the soaking process. The sample carbon foam was soaked for 30 seconds inside the water-oil emulsion. Then the sample of carbon foam was weighed again to get the final weight. The weighing process was run by using the laboratory balance equipment. The oil adsorption capability of the carbon foam will be calculated by using The Equation (3) below [12].

$$Oil\ Absorption\ Capability\ (\%) = \left(\frac{mf - mi}{\text{mi}}\right) \times 100 \quad (3)$$

mi = initial weight of sample (kg)
mf = final weight of sample (kg)

2.6 Reusability

The reusability test was conducted to observe the usable cycle by burning the oil-filled carbon foam. The carbon foam was soaked inside the petroleum oil to create the oil-filled carbon foam and burn it directly in the air [13]. The foam will be burned for 30 seconds. The characteristics of the carbon foam will be observed by the shape and surface structure profile. The process was done by using the butane torch inside fume hood.

3. Results and Discussion

3.1 Density and Porosity

The bulk density and percentage porosity of the carbon foam were calculated according to the Archimedes Principle. The data taken are the dry weight, submerged weight and wet weight of the samples. Based on Fig. 2(a), the CFE had the maximum bulk density which is 0.2625 g/cm^3 and the CFA had the minimum bulk density which is 0.2235 g/cm^3. The pattern graph of the bulk density increases from CFA to CFE. The value of bulk density increases when the amount of carbon powder increases. It shows that the relationship between the amount of carbon powder and bulk density is directly proportional.

From Fig. 2(b), for the porosity percentage of the carbon foam, the result obtained for the graph is in decreasing pattern. The maximum porosity is 83.67% which is obtained by CFA and CFE had the minimum porosity which is 81.73%. The increase amount of carbon powder affected the porosity percentage of the carbon foam where it becomes decrease. It shows the indirectly proportional relationship between the amount of carbon powder and the porosity percentage. The relationship between the bulk density and porosity percentage are indirectly proportional where the more the bulk density, the less the porosity percentage of the carbon foam.

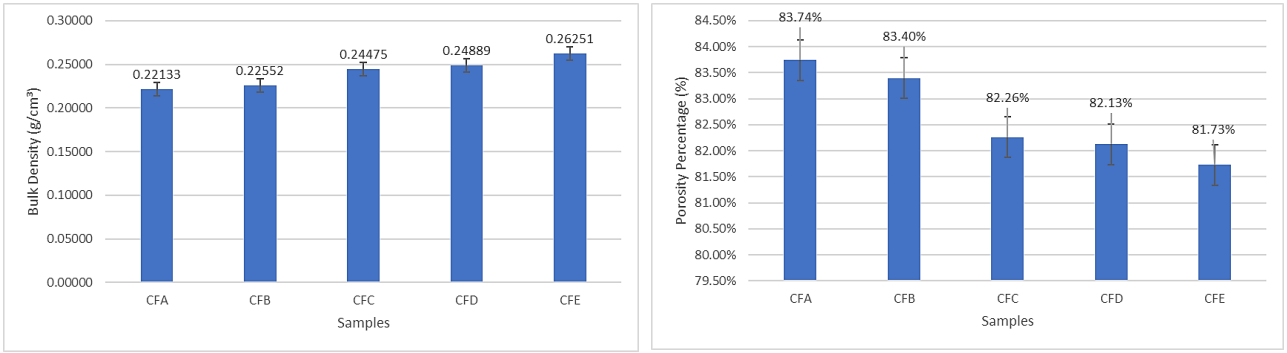

(a) **(b)**

Fig. 1 *The graph of (a) bulk density; (b) porosity percentage of carbon foam*

3.2 Pore Morphology Observation

Pore morphology was discovered inside of the carbon foams by using the Scanning Electron Microscope (SEM to identify the relationship between pore size and presence of the carbon powder. From Fig. 2, clearly observed that CFA had the biggest size of the pore while the carbon foam that contained of carbon powder had the tighter size of the pore. It can be observed that the most percentage amount of carbon powder had smaller size of pores. It obviously seemed that CFE had the tight microstructure and the smallest size of pore. The average pore size for CFA is around 27.6 µm. Meanwhile, the CFA had the largest pore size with average pores size around 92µm. Beside microspores, macropores also clearly was observed in CFA. The size of macropores was measured around 0.32mm. Furthermore, observation on CFB, CFC and CFD show that the presence of the carbon powder in CFB, CFC, CFD makes the pore becomes smaller and tight. The pore size of CFB was recorded about 63.1 µm and some macropores also still can be observed. However, the size of macropores was decreased to 0.15mm. Furthermore, the measured pore size for CFC and CFD were recorded around 43.7 µm and 37.6 µm respectively. It is expected that the presence of the carbon powder will cover the gap of the pore and thicken the pore wall resulted to reduce the size of pores. The presence of the carbon powder inside the pore of the carbon foam was proven in the Fig. 3.

Int. Journal of Integrated Engineering Vol. 17 No. 8 (2025) p. 65-77

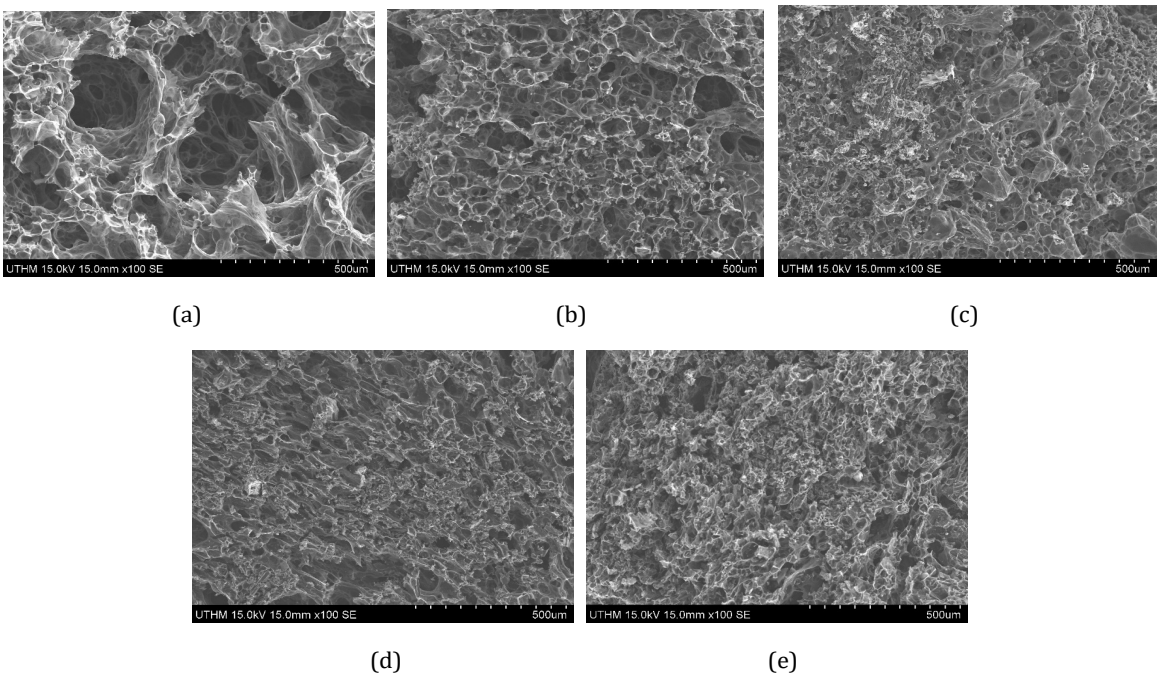

Fig. 2 *Pore distribution under 100x of magnification; (a) CFA (0wt%); (b) CFB (2wt%); (c) CFC (4wt%); (d) CFD (6wt%); (e) CFE (8wt%)*

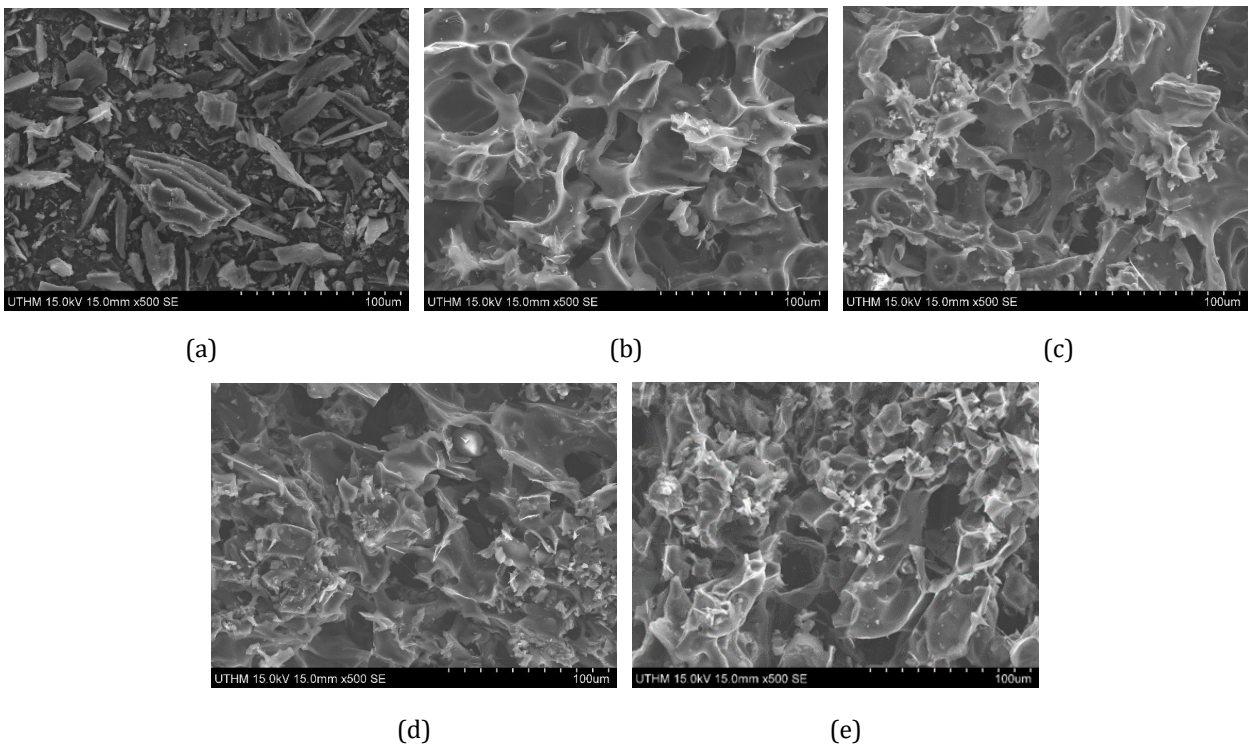

Fig. 3 *Morphology of samples under 500x of magnification; (a) CFA (0wt%); (b) CFB (2wt%); (c) CFC (4wt%); (d) CFD (6wt%); (e) CFE (8wt%)*

From Fig. 3, it observed the presence of the carbon powder of each sample. The shape of the carbon powder is the same as the inside microstructure of the carbon foam. It indirectly increases the cell wall thickness and bulk density but decreases the porosity of the carbon foam. From the result obtained, it can be proved by the density and porosity test where the density increases when the presence of the carbon powder increases. The porosity of

the carbon foam decreases as the amount of carbon powder increases. It indicates that the addition of carbon powders has a clear effect on cell morphology in terms of cell-wall thickness, pore-section diameter, and foam density [14].

3.3 Elemental Analysis

The element of the carbon foam was done by Energy Disperse X-Ray (EDX) attached in SEM. The selected spectrum analysed is the pore wall. The results obtained overall are the percentage of carbon, oxygen and natrium as shown in EDX spectrum in Fig. 4 until Fig. 8. Carbon is obviously the highest percentage for all the samples. The presence of the sodium element was coming from the sodium borate that was used as the blowing agent. From the summarized results obtained in Figure 9, the percentage of carbon for CFE was the maximum, which is 95.79%. The presence of oxygen and sodium was very little compared to the minimum content of carbon CFA. CFA had the highest percentage element of oxygen and sodium which are 7.19% and 1.33%. CFB, CFC and CFD also had a higher percentage of carbon compared to CFA and it is increasing until CFE. It increased from 92.60% to 93.31%, then up to 94.46%. The element percentage was different for each sample due to the addition of the carbon powder. The percentage element of carbon increases as the amount of the carbon powder increase. As the amount of carbon increases, the density of the carbon foam increases and the porosity of the carbon foam decreases.

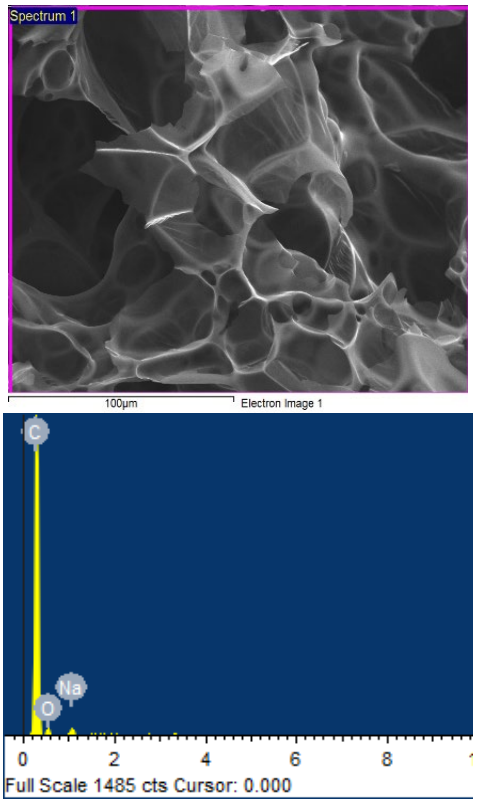

Fig. 4 *EDX spectrum of CFA (0wt% of carbon powder)*

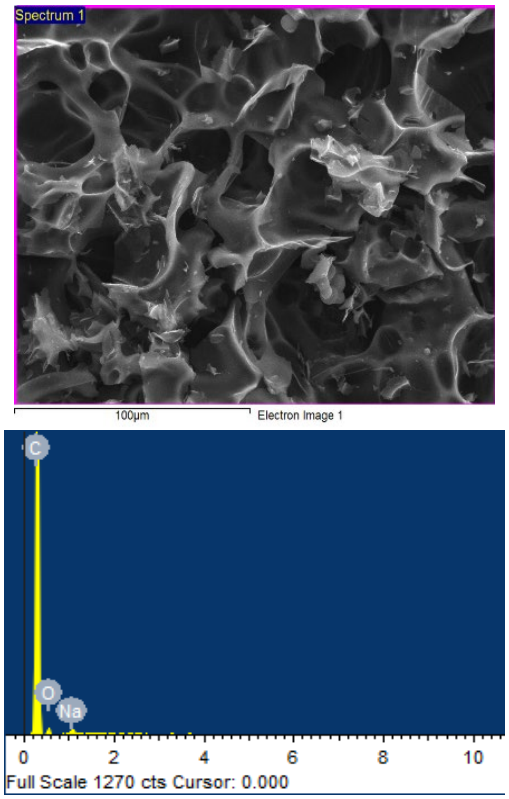

Fig. 5 *EDX spectrum of CFB (2wt% of carbon powder)*

Int. Journal of Integrated Engineering Vol. 17 No. 8 (2025) p. 65-77

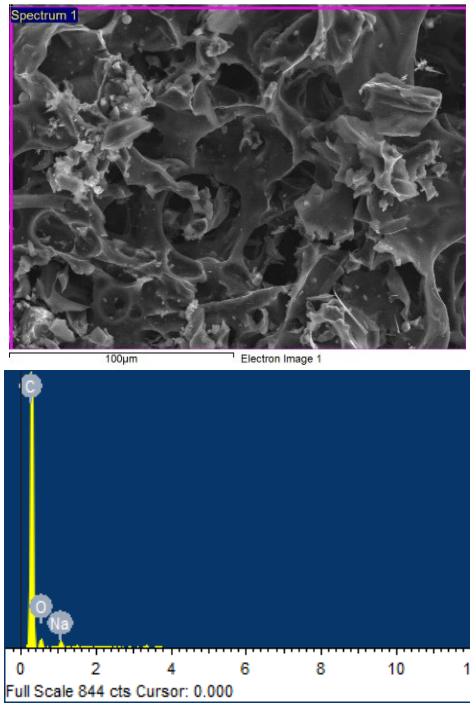

Fig. 6 *EDX spectrum of CFC (4wt% of carbon powder)*

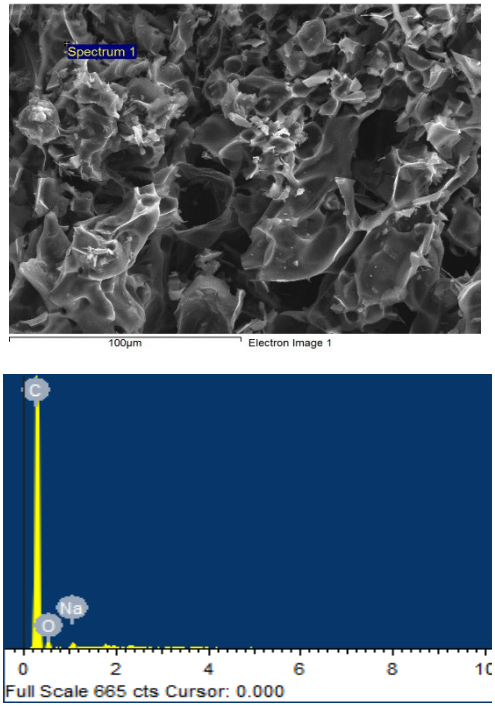

Fig. 7 *EDX spectrum of CFD (6wt% of carbon powder)*

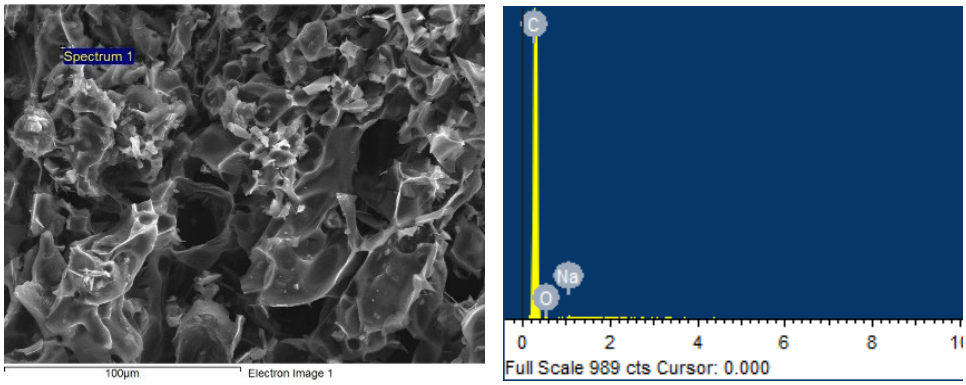

Fig. 8 *EDX spectrum of CFE (8wt% of carbon powder)*

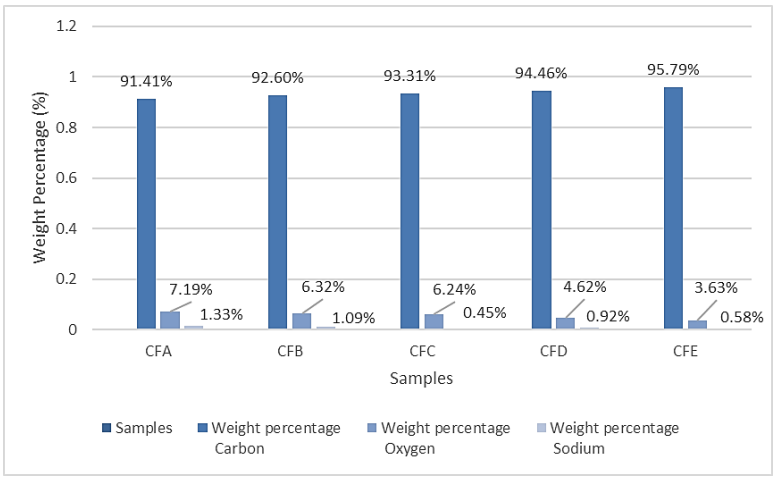

Fig. 9 *Graph of elemental percentage of carbon foam*

3.4 FTIR

In this study, it was used to identify the functional group element in raw material and foaming carbon for each parameter. The observation was done by using a Fourier-infrared Spectroscopy (FTIR) machine. The starch, sample before foaming and carbon foam were crushed into powder structure before the testing began. The results obtained were compared between raw and foaming carbon for each parameter from 600 cm^{-1} to 4000 cm^{-1}. The red circles indicate the wavenumbers of functional group element presence for raw material and yellow circles for carbon foam. Fig. 10 shows the FTIR analysis spectrum for starch and Fig. 11 shows the FTIR analysis for all carbon foam.

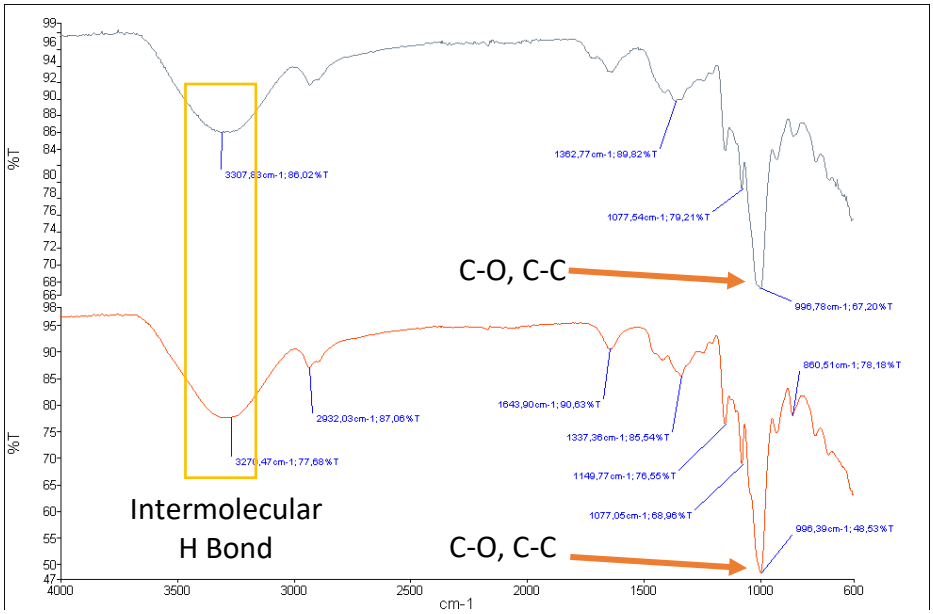

Fig. 10 *FTIR analysis spectrum of starch (black spectrum) and sample before foaming (red spectrum)*

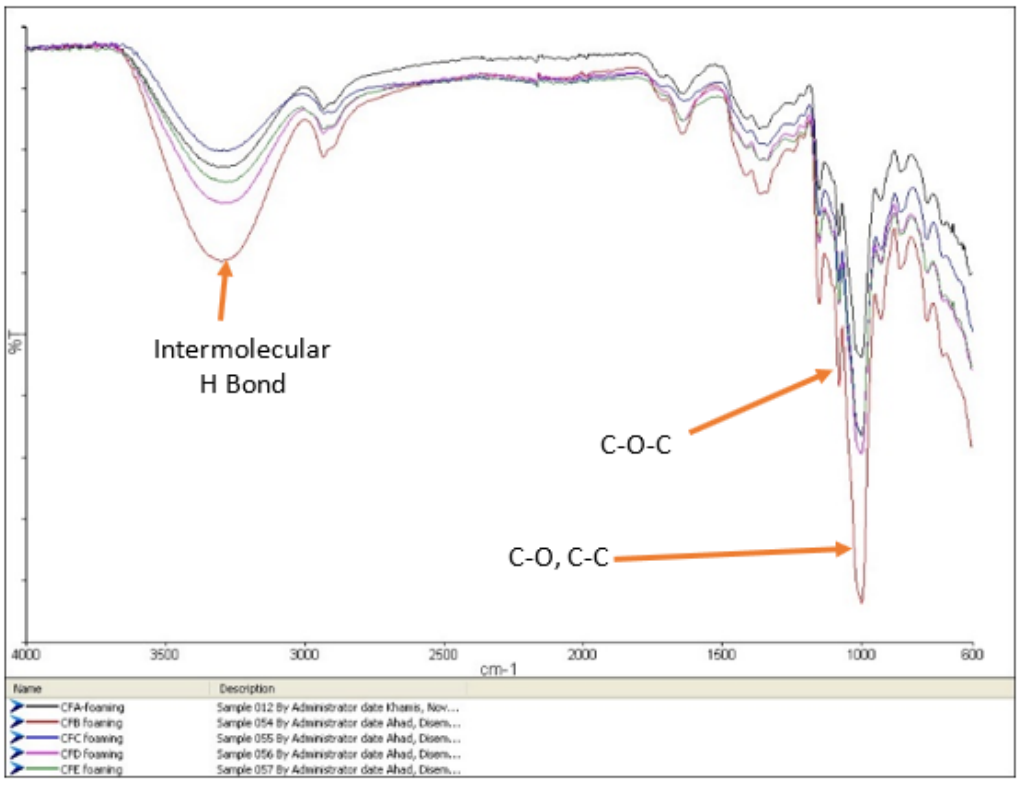

Fig. 11 *FTIR analysis spectrum of carbon foams*

Int. Journal of Integrated Engineering Vol. 17 No. 8 (2025) p. 65-77

Based on observation at range 3200 cm^{-1} to 3550 cm^{-1} in Figure 10 and 11, all parameters which are starch, sample before foaming and carbon foam show the intermolecular H bonds. The maximum wavenumber of intermolecular H bonds was 3307.83 cm^{-1} obtained by carbon foam with no carbon powder. The pattern for all parameters increases from their raw materials. For the carbon foam, the intensity becomes higher due to the foaming process and the presence of water during the mixing process. Another wavenumber that observed is between 1070 cm^{-1} to 1300 cm^{-1}, which is where the C-O-C vibrations. The bands at 1144 cm^{-1} and 926 cm^{-1} correspond to C-O stretching and C-C skeletal mode vibration, respectively [15]. The wavenumber for all the materials and parameter in between 1077.54 cm^{-1} to 1076.75 cm^{-1} and the maximum value obtained by carbon foam with no carbon powder. The characteristic peaks of starch-containing models are at 1010 cm^{-1}, 1080 cm^{-1}, and 1150 cm^{-1}. These are attributed to the polysaccharide molecules' combined C-O and C-C stretching vibrations [16]. The intensity started to decrease as the reinforcement, carbon powder started mixed with the starch. It is because the molecules were lost when more carbon powder mixed with starch. Besides that, the trend also shows the carbon foams were higher than its raw material. It is because more carbon content after the foaming process and it is where the carbonization occurred. For 990 cm^{-1} to 1060 cm^{-1}, it shows the characteristic bands of C-OH stretching vibration which is secondary cyclic alcohol. From the results obtained for all parameters, the intensity of the foaming carbon is higher than the raw materials. It was due to carbonization and more presence of carbon atoms.

3.4 Compression

The compression test was carried out to determine the carbon foam's behaviour when constant force applied on the carbon foam. Fig. 12 shows the carbon foam's condition before and after compression test. While Fig. 13 is the graph obtained for average maximum stress and average maximum strain.

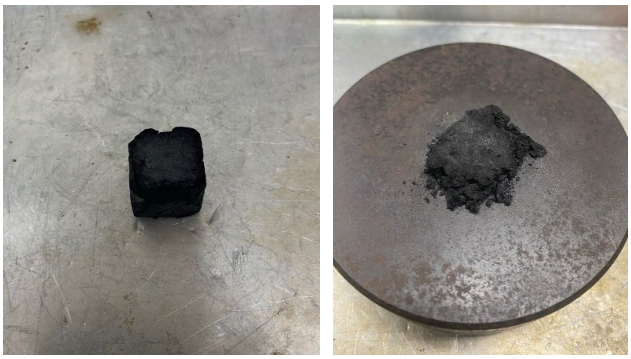

(a) **(b)**

Fig. 12 *Figure of carbon foam (a) before; and (b) after compression*

From Fig. 13(a), the highest value of maximum stress was achieved by CFE which is 1.71345 N/mm^2. The properties of the carbon foam decrease as the content of the carbon powder decreases from the graph. The lowest value of maximum stress was obtained by CFA which is 0.51743 N/mm^2. It is due to the more porosity contained inside the samples and no presence of carbon powder that can reinforce the carbon foam. CFA also had the lowest density among the other samples.

Based on Fig, 13(b), the highest is CFE which is 302.79167N and the lowest is 91.43750N that was obtained by CFA. The CFA had much porosity and low bulk density that affected the value of the maximum force. No presence of carbon powder also one of the factors that affected the carbon foam when the force applied. Besides that, when the highest presence of carbon powder in CFE, the maximum force value became the highest because it can increase the mechanical properties of the carbon foam and withstand when the high force applied. It can conclude that, the more the carbon powder contained inside the carbon foam, the more the stress value and force can be applied. It is due to the carbon powder that increase the bulk density and decrease the porosity of the carbon foam. The compressive strength of the samples containing carbon powder increases as the pore cell density of the sample increases. It is reported by Narasimman, R. et.al, that the compressive strength of carbon foam was influenced by density, porosity and the type of reinforcement used [17]. Furthermore, it is expected that the carbon powder embedded on the wall surface was prevent microcrack propagated and resulted to increase the strength of the wall [18].

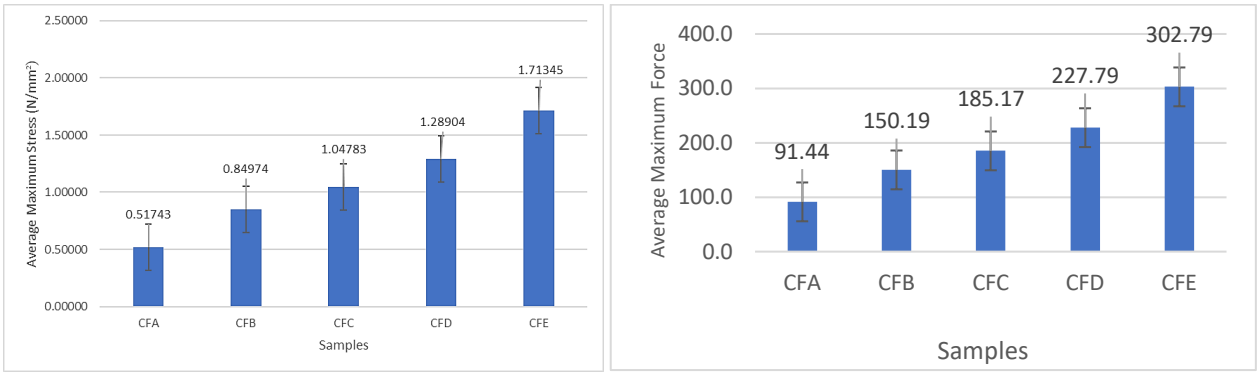

(a) **(b)**

Fig. 13 *The graph of compression test (a) average max. stress vs samples; (b) average max. force vs samples*

3.4 Oil Absorption Study

The oil adsorption performance was observed through the adsorption process as shown in Fig. 14 which shows the before, during and after soaking process. It is clearly shown that the oil was absorbed into the carbon foam where the emulsifier was dismissed after the soaking process. Meanwhile Fig. 15 shows the graph for the oil adsorption of every sample.

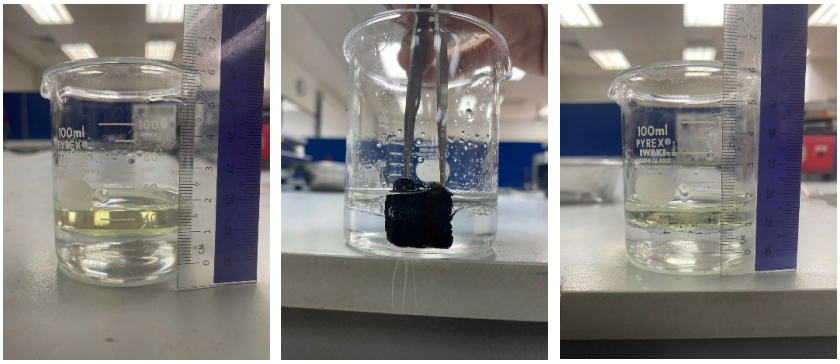

(a) **(b)** **(c)**

Fig. 14 *Observation of oil absorption (a) before soaking; (b) during soaking; (c) after soaking*

Besides observation through eyes, the amount of oil absorbed into the carbon foam was also calculated and shown in graph of Fig. 15. From the graph, the highest percentage of adsorption was achieved by CFA which is 275.80% while the lowest percentage is 87.37 that was achieved by CFE. The trend of the bar chart is decreasing as the amount of carbon powder increases. CFB and CFC also had higher percentage of oil adsorption but not as low as CFD and CFE. When the amount of carbon powder and density increases, the adsorption capabilities are totally against the CFA which is low. Low porosity also affected the oil adsorption capability such as CFE which had the lowest percentage of oil adsorption. It is due to the presence of carbon powder and the highest bulk density. Carbon has the capability to absorb the oil due to its surface properties [19]. It can be concluded that the highest porosity of carbon foam achieves the highest percentage of oil absorption. The relationship between the amount of carbon powder and oil adsorption is indirectly proportional due to the bulk density of carbon foam.

Int. Journal of Integrated Engineering Vol. 17 No. 8 (2025) p. 65-77

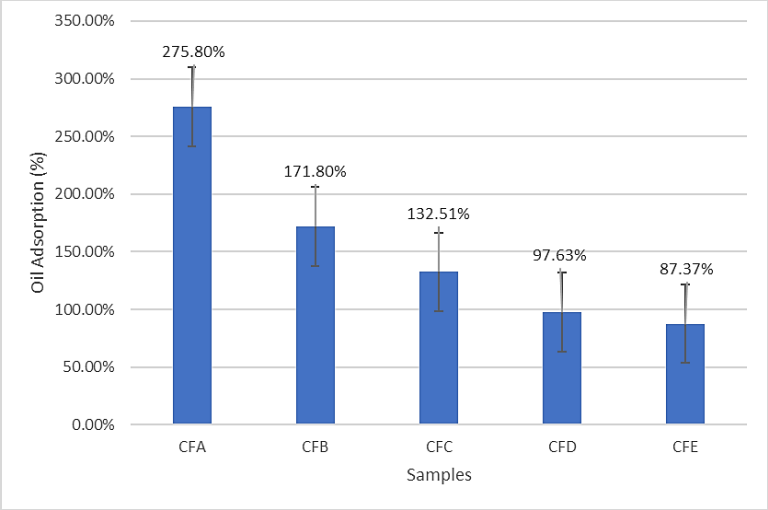

Fig. 15 *Percentage of oil adsorption for different samples*

3.4 Reusability Study

The reusability test was conducted to observe the usable cycle by burning the oil-filled carbon foam. The foam will be burned for 30 seconds. The characteristics of the carbon foam will be observed by the shape and surface structure profile. The process was done by using the butane torch inside fume hood. After the burning of the carbon foam, there were not many differences compared to the original samples. The shape of the samples remains the same, but the surface colour became grey, and the edges colour became darker. The structure profile is still consistent, and the results obtained are the same for all parameters. The outer physical for all the samples did not damage when they were burned for 30 seconds even though the embers were still at the surface of the samples after the burning finished. All the samples can withstand the burning for 30 seconds with the petrol oil inside the pore. Indirectly, the carbon foam can perform well in a hot environment, and it can be reused if the burning happens. This is indicated that the carbon foam is fire retardant due to its thermal stability and low coefficient of thermal expansion [20]. Fig. 16 shows the before, during and after the burning process.

(a) **(b)** **(c)**

Fig. 16 *The condition of the samples (a) before burning; (b) during burning; (c) after burning*

4. Conclusion

In this study, the main objectives of this research were accomplished with the complete analysis. The starch-based carbon foam reinforce with carbon powder was fabricated with five different parameters. The effect of the carbon powder for physical and mechanical properties was carried out though the experimental test. The density and porosity test was done and was observed that the bulk density of the carbon foam increases as the carbon powder percentage increases. This also affected the porosity of the carbon foam where the porosity increases when the carbon powder percentage decreases. For pore morphology, it was observed that the higher the carbon powder content, the higher the presence of carbon powder at pore wall but low pore size. The FTIR analysis shows the

carbon content also increases from raw material after the foaming process for every parameter. The wavenumbers also higher for the foaming carbon might be due to carbonization and more presence of carbon atoms. The density of the carbon foam affected the compression results, and the reinforcement enhances the mechanical properties of the carbon foam. The maximum stress value and maximum force applied are higher when more amount of carbon powder is added. The reusability test concluded that carbon foam can perform well in a hot environment, and it can be reused if burning happens. Besides making the carbon foam denser and stronger, the carbon powder weakened the oil adsorption ability. The more the presence of the carbon powder, the lower the oil adsorption abilities. The oil adsorption must be excellent but in terms of the mechanical properties also must perform well especially at the outside environment. So, the CFC had the best properties that can perform both mechanical properties and oil adsorption.

Acknowledgement

This research was supported by Ministry of Higher Education Malaysia through Fundamental Research Grant Scheme (FRGS/1/2018/TK03/UTHM/03/9). We also want to thank to Universiti Tun Hussein Onn Malaysia (UTHM) for sponsoring this work under research grant No. K050.

Conflict of Interest

The authors declare that there is no conflict of interest regarding the publication of the paper.

Author Contribution

The authors are responsible for the study conception, research design, data collection, data analysis, result interpretation and manuscript drafting.

References

[1] Banerjee, C., Chandaliya, V. K., Dash, P. S., & Meikap, B. C. (2019). Effect of different parameters on porosity and compressive strength of coal tar pitch derived carbon foam. *Diamond and Related Materials*, 95, 83–90. https://doi.org/10.1016/j.diamond.2019.04.009

[2] Yu, M., Li, C., Ao, X., & Chen, Q. (2019). Fabrication of coal tar pitch–derived reticulated carbon foam as oxidation-resistant thermal insulation. *Journal of Analytical and Applied Pyrolysis*, 141, 104643. https://doi.org/10.1016/j.jaap.2019.104643

[3] M., Zefeng, J., Chenchen, F., Mingzheng, Q., & Donghai, X. (2023). Research and development progress of porous foam-based electrodes in advanced electrochemical energy storage devices: A critical review." *Renewable and Sustainable Energy Reviews*, 173, 131111. https://doi.org/10.1016/j.rser.2022.113111

[4] Mahdi, M., Negin, S., Hossein, K., Rouhollah, A., Parisa, A, Reza, S., & Alireza, V. (2023). Electro-driven carbon foam/PCMs nanocomposites for sustainable energy management. *Journal of Energy Storage*, 67, 107599. https://doi.org/10.1016/j.est.2023.107599

[5] Chang-Gu, L., Mi-Kyung, S., Jae-Chun, R., Chanhyuk, P., Jae-Woo, C., & Sang-Hyup, L. (2016). Application of carbon foam for heavy metal removal from industrial plating wastewater and toxicity evaluation of the adsorbent. *Chemosphere*, 153, 1-9. https://doi.org/10.1016/j.chemosphere.2016.03.034

[6] Yang, S., Wang, F., Tang, Q., Wang, P., Xu, Z., & Liang, J. (2019). Utilization of ultra-light carbon foams for the purification of emulsified oil wastewater and their adsorption kinetics. *Chemical Physics*, 516, 139–146. https://doi.org/10.1016/J.CHEMPHYS.2018.08.051

[7] Qidong, W., Jiayi, Z., Fangjun, Y., Yunyan, L., Ye, Z., Xiangwen, P., Donghuan, H., Siyi, Z, Weihong, Z., Jizhen, S., Shuai, L., Hua, W, Yu, S., Hiroshi, U., & Guojiang M. (2023). A thermoplastic polyurethane-based composite aerogel with low shrinkage and high specific surface area enhanced by activated carbon for highly efficient oil/water separation. *Journal of Environmental Chemical Engineering*, 11(5), 111077. https://doi.org/10.1016/j.jece.2023.111077

[8] Anushi, S., Ashutosh, P., Veerendra, K. P., Neelam, S., Hemant, J., Anup, K., Neeraj, D., Gaurav, G., Mondal, D.P., Srivastava, A.K., Rajeev K. (2023). Sustainable lightweight multifunctional carbon foams derived from coal tar pitch using urea as a pore-forming agent. *Journal of Analytical and Applied Pyrolysis*, 174, 106145. https://doi.org/10.1016/j.jaap.2023.106145

[9] Kim, Y., Kim, J. K., Vaalma, C., Bae, G. H., Kim, G. T., Passerini, S., & Kim, Y. (2018). Optimized hard carbon derived from starch for rechargeable seawater batteries. *Carbon*, 129, 564–571. https://doi.org/10.1016/j.carbon.2017.12.059

[10] Xuan, S., Tian, Y., Kong, X. Y., Hao, J., Wang, X. (2023). Effect of different MgO/Al2O3 ratios on microstructural densification, sintering process and mechanical property of MgAl2O4 materials. *Journal of Materials Research and Technology*, 25, 2518-2526 https://doi.org/10.1016/j.jmrt.2023.06.044

[11] Zikang, P., Jiangang, J., Jiakang, J., Chao, N., Diqiang, L. (2023). Fabrication and characterization of glassy carbon foams with controllable porosity and high compressive strength. *Diamond and Related Materials*, 138, 110256. https://doi.org/10.1016/j.diamond.2023.110256

[12] Hongfu, Z., Ruijing, M., Linyan, W., Min, Z., Xinyi, W., Xiangdong, W., Jing, H. (2024). Preparation of open-cell chain-extend poly (lactic acid)/poly (butylene adipate-co-terephthalate) foams and their selective oil absorption characteristics. *The Journal of Supercritical Fluids*, 204, 106114. https://doi.org/10.1016/j.supflu.2023.106114

[13] Vannarath, A., & Thalla, A. K. (2021). Synthesis and characterisation of an ultra-light, hydrophobic and flame-retardant robust lignin-carbon foam for oil-water separation. *Journal of Cleaner Production*, 325, 129263. https://doi.org/10.1016/J.JCLEPRO.2021.129263

[14] Li, W. Q., Zhang, H. B., Xiong, X., & Xiao, F. (2011). A study of the properties of mesophase-pitch-based foam/graphitized carbon black composites. *Materials Science and Engineering: A*, 528(6), 2999–3002. https://doi.org/10.1016/j.msea.2010.12.013

[15] Fonseca-Florido, H. A., Yañez-Macías, R., Ávila-Orta, C. A., Cruz-Delgado, V. J., & Covarrubias-Gordillo, C. A. (2024). Starch/carbon nanofibers bionanocomposites via melt mixing: Effect of dispersion and compatibility on conductivity and mechanical properties. *International Journal of Biological Macromolecules*, 256, 128519. https://doi.org/10.1016/j.ijbiomac.2023.128519

[16] Pourfarzad, A., Yousefi, A., & Ako, K. (2021). Steady/dynamic rheological characterization and FTIR study on wheat starch-sage seed gum blends. *Food Hydrocolloids*, 111, 106380. https://doi.org/10.1016/j.foodhyd.2020.106380

[17] Narasimman, R., & Prabhakaran, K. (2013). Preparation of carbon foams with enhanced oxidation resistance by foaming molten sucrose using a boric acid blowing agent. *Carbon*, 55, 305-312. https://doi.org/10.1016/j.carbon.2012.12.068

[18] Hassan N. Z., Nasrul, Hatta, M., Badarulzaman, M., Farahin, N. A., & Joharudin, M. (2022). The Effect of Graphite Loading as Reinforcement on Carbon Foam from Natural Resources. *Technology Reports of Kansai University*, 908, 9–13. https://doi.org/10.4028/p-tsffu3

[19] Shiqi, W., Daming, C., Guangdong, Z., Yuan, C., Boqian, S., Xiaojie, Y., Wenbo, H., Guiqing, C, Xinghong, Z. (2022). Controllable synthesis of a robust sucrose-derived bio-carbon foam with 3D hierarchical porous structure for thermal insulation, flame retardancy and oil absorption. *Chemical Engineering Journal*, 434, 134514. https://doi.org/10.1016/j.cej.2022.134514

[20] Rajeev, K., Hemant, J., Anisha, C., Saroj, K., Mondal D.P., Srivastava, A.K. (2019). Thermal conductivity and fire-retardant response in graphite foam made from coal tar pitch derived semi coke. *Composites Part B: Engineering*, 172, 121-130. https://doi.org/10.1016/j.compositesb.2019.05.036